J Comput Aided Mol Des (2012) 26:349–361
DOI 10.1007/s10822-012-9561-2

Computer-aided design of novel antibacterial 3-hydroxypyridine-4-ones: application of QSAR methods based on the MOLMAP approach

Razieh Sabet · Afshin Fassihi · Bahram Hemmateenejad · Lotfollah Saghaei · Ramin Miri · Maryam Gholami

Received: 10 December 2011 / Accepted: 8 March 2012 / Published online: 28 March 2012

Abstract 3-Hydroxypyridine-4-one derivatives have shown good inhibitory activity against bacterial strains. In this work we report the application of MOLMAP descriptors based on empirical physicochemical properties with genetic algorithm partial least squares (GA-PLS) and counter propagation artificial neural networks (CP-ANN) methods to propose some novel 3-hydroxypyridine-4-one derivatives with improved antibacterial activity against *Staphylococcus aureus*. A large collection of 302 novel derivatives of this chemical scaffold was selected for this purpose. The activity classes of these compounds were determined using the two quantitative structure activity relationships models. To evaluate the predictability and accuracy of the obtained models, nineteen compounds belonging to all three activity classes were prepared and the activity of them was determined against *S. aureus*. Comparing the experimental results and the predicted activity classes revealed the accuracy of the obtained models. Seventeen of the nineteen synthesized molecules were correctly predicted by GA-PLS model according to the antimicrobial evaluation method. Molecules **5f** and **5h** proved to be moderately active and active experimentally, but were predicted as inactive and moderately active compounds, respectively by this model. The CP-ANN based prediction was correct for sixteen out of the nineteen synthesized molecules. **5a**, **5h** and **5q** were moderately active and active based on the antimicrobial assays, but they were introduced as members of inactive, moderately active and inactive classes of compounds, respectively according to CP-ANN model.

Keywords Antibacterial activity · CP-ANN · 3-Hydroxypyridin-4-one · MOLMAP · QSAR

Abbreviations

ANN	Artificial neural networks
CP-ANN	Counter propagation artificial neural networks
2D	Two dimensional
3D	Three dimensional
GA-PLS	Genetic algorithm partial least squares
MIC	Minimum inhibitory concentration
MLR	Multiple linear regression
MOLMAP	Molecular map of atom-level properties
SOM	Self-organizing maps
QSAR	Quantitative structure activity relationships

Introduction

Iron is one of the trace elements inevitably required for the survival and proliferation of all living things [1]. Pathogenic bacteria require iron to proliferate and cause infectious diseases in the human body. Vertebrate hosts withhold iron

Electronic supplementary material The online version of this article (doi:10.1007/s10822-012-9561-2) contains supplementary material, which is available to authorized users.

R. Sabet · A. Fassihi (✉) · L. Saghaei
Department of Medicinal Chemistry, School of Pharmacy and Pharmaceutical Sciences and Isfahan Pharmaceutical Research Center, Isfahan University of Medical Sciences, Isfahan, Iran
e-mail: fassihi@pharm.mui.ac.ir

R. Sabet
Department of Medicinal Chemistry, Faculty of Pharmacy, Shiraz University of Medical Sciences, 7146864685 Shiraz, Iran

B. Hemmateenejad (✉) · R. Miri · M. Gholami
Medicinal & Natural Product Chemistry Research Center, Shiraz University of Medical Sciences, Shiraz, Iran
e-mail: hemmatb@sums.ac.ir

from microbial invaders as a major defence mechanism against infection [2]. Many bacteria synthesize small molecules known as siderophores, which possess high affinity to iron and scavenge it from the environment [3]. 3-Hydroxypyridine-4-one derivatives and their oxygen-containing analogues, 3-hydroxypyran-4-ones, belong to a class of iron chelators with reported in vitro antibacterial, antifungal and antimalarial activities [4–7]. They have shown inhibitory effects on the growth of *Escherichia coli*, *Listeria inocua* and *Staphylococcus aureus* [8–10]. We have previously reported the antimicrobial activities of novel Mannich bases of 2-alkyl-3-hydroxy-pyridine-4-ones as well as 1-alkyl substituted 2-alkyl-3-hydroxypyridine-4-ones. They have shown inhibitory effects on the growth of *S. aureus, Salmonella enteritidis* and *Aspergillus flavus* [11].

Quantitative structure activity relationships (QSAR) approach has been widely developed because of its powerful ability to predict drug activity [12]. QSAR models are mathematical equations relating chemical structures to their biological activities. Various methods have been applied to construct QSAR models including linear and nonlinear regression methods. Multiple linear regression (MLR) and artificial neural networks (ANN) have been extensively employed in QSAR studies owing to their outstanding linear and nonlinear mapping capability, respectively [13, 14]. Appropriate application of the structural and physicochemical features of molecules is an essential key to achieve successful QSAR models [12]. Nowadays, a multi-way analytical method based on Kohonen network, originated from a method for calculation of molecular descriptors called MOLMAP (molecular map of atom-level properties), has been introduced [15–17]. Kohonen self-organizing maps (SOM) are a class of unsupervised neural networks whose characteristic feature is the reduction of multidimensional data to 2 dimensional (2D) ones [18]. In QSAR modeling based on MOLMAP approach, the resulted Kohonen scores are used as descriptors for classification and regression purposes.

The chemical reactivity of a compound, being related to the ability to make and break bonds, primarily depends on the properties of the bonds available in a molecule. Gasteiger et al. proposed that seven empirical physicochemical properties are particularly relevant for representing bonds and for modeling chemical reactivity [19]. These properties are calculated by empirical procedures implemented in PETRA program [20]. To explore all that information for an entire molecule, and simultaneously have a fixed-length representation, they proposed to map all the bonds of a molecule into a fixed-length 2D SOM: a *MOLMAP* [21]. A SOM must be trained previously with a diversity of bonds from different structures (each bond described by the seven bond properties) [18]. Then, all the bonds of one molecule are submitted to the trained SOM, each bond activates one neuron, and the pattern of activated neurons is a map of the reactivity features of that molecule (MOLMAP) as a fingerprint of the bonds available in that structure.

Regression models for a series of 3-hydroxypyrane-4-one and 3-hydroxypyridine-4-one derivatives have been previously investigated by our research group [11, 22]. According to these studies the most significant QSAR models were obtained by GA-PLS against *S. aureus*. Sometimes biological data can be classified into discrete categories. For example, a chemical may be classified as either active or inactive, or in several classes according to the potency of the activity. In such cases, other statistical techniques, such as classification methods must be applied, in which the physicochemical properties of the compounds are used to discriminate between activity and inactivity.

In this paper, we used the PETRA 3.20 software package to calculate empirical physicochemical properties of bonds, and MOLMAP descriptors were generated on the basis of the bond properties [19, 20]. These descriptors were applied with GA-PLS and CP-ANN methods to propose some novel 3-hydroxypyridine-4-one derivatives with improved antibacterial activity against *S. aureus*. The proposed compounds were prepared in the lab and their antibacterial potency was evaluated. The reason for selecting this microorganism and this chemical scaffold was the good diversity in the antimicrobial potencies observed in our previously reported studies. Significant GA-PLS models have described the effect of structural modification of this scaffold and anti *S. aureus* activity too [11, 22]. We performed the computational part of the study on a large collection consisted of 302 novel derivatives of 3-hydroxypyridine-4-one. Most of these compounds have not been prepared experimentally yet and none were evaluated as antimicrobial agents previously. It is well known that the hydrazone group plays an important role for the antimicrobial activity in many different scaffolds. Furthermore, a number of acylhydrazone derivatives have been demonstrated to possess interesting antibacterial, antifungal [23], antimalarial [24] and antitubercular activities [25]. Schiff's bases have also been shown to exhibit a broad range of biological activities, including antiviral, antimalarial, antifungal and antibacterial properties [26, 27]. Thus, the antimicrobial capacity of hydrazide-hydrazone and Schiff's base moieties was considered in the design of these compounds.

Materials and methods

QSAR analysis

The experiments described here required two major steps: generation of descriptors and development of predictive

models. To generate the descriptors, some properties were processed by a Kohonen SOM to MOLMAPs scores [18]. For training this map, each object of the training set was a chemical bond, each bond represented by seven empirical physicochemical properties. This training set contains bonds from diverse structures. Once trained, the map is used to obtain molecular descriptors. Bonds of one molecule were submitted to the trained SOM, and the pattern of activated neurons, which is a map of the reactivity features of that molecule (MOLMAP), is the descriptor of the molecule. The second step consisted of establishing relationships between MOLMAP descriptors and antimicrobial activity against *S. aureus*.

Data set

A set of thirty-one 3-hydroxypyridine-4-one and 3-hydroxypyran-4-one derivatives was compiled from literature and our previous reports [4, 5, 11]. The antimicrobial activity (against *S. aureus*) was reported as MIC. Different strains of this microorganism were used in these reports: PTCC 1337, ATCC 25923, and PTCC 29213. It was assumed that there will be no big differences between the susceptibility of these different strains and the strain applied in the present study (PTCC 1112) against the antimicrobial activity of the studied compounds. The molecules were classified as active (class 1) if they exhibited 8 μg/mL $\leq$ MIC $\leq$ 32 μg/mL (3 molecules); moderately active (class 2) if 64 μg/mL $\leq$ MIC $\leq$ 128 μg/mL (9 molecules) and inactive (class 3) if MIC was more than 128 μg/mL (19 molecules). The structural features, biological activity and the class of these compounds are listed in Table 1.

Training of a Kohonen self-organizing map with empirical physicochemical descriptors

Kohonen SOM is an unsupervised neural network that reveals similarities between objects. It can be used for the reduction of multidimensional objects to two dimensional objects. In this study, we used SOMs to reduce the dimensions of chemical bonds, represented by seven empirical physicochemical bond properties calculated by PETRA to 2D data. A Kohonen SOM consists of a grid of so-called neurons, each containing as many elements (weights) as input variables. Figure 1s shows the architecture of a Kohonen network. Here the objects are bonds, and the input variables are the seven properties of bonds. Before the training starts, the weights take random values. During the training, each individual bond is mapped into the neuron that contains the most similar weights compared to its properties. This is the central neuron, or winning neuron [18]. The winning neuron was activated by the bond, and its weights were then adjusted to make them even more similar to the properties of the presented bond. Not only the winning neuron, but also the neurons in its neighborhood have their weights adjusted. The extent of adjustment depends, however, on the topological distance to the winning neuron, the closer a neuron is to the central neuron the larger is the adjustment of its weights. The objects of the training set are iteratively fed to the map, the weights corrected, and the training is stopped when a predefined number of cycles are attained. A trained Kohonen SOM will reveal similarities in the objects of a data set in the sense that similar objects (similar bonds) are mapped into the same or closely adjacent neurons [18]. Figure 1s is shown in the supplementary materials.

Molecular descriptors

Chemical bonds were represented by seven empirical physicochemical bond properties calculated by PETRA 3.20. These properties were the difference of σ electronegativity between the two atoms of the bonds, difference of π atomic charges, difference of total atomic charges, bond polarity, mean bond polarizability, resonance stabilization, and bond dissociation energy. As some properties depend on the orientation of the bond, each bond was represented as (A–B) [21]. Figure 1 shows the common bonds (11 bonds) in the molecules and the numbers assigned to the bonds. A three-dimensional array of empirical physicochemical parameters (molecules, bonds and the empirical physicochemical properties on each dimension, a 333 $\times$ 11 $\times$ 7 array) was provided (Fig. 1). Then, the pattern of the activated neurons can be considered as a fingerprint of the objects and constitute their MOLMAP scores [18]. At last; the map is transformed into a vector by concentration of columns resulting in a fixed length MOLMAP score where each scores of each object have a dimension of ($N \times N$). The best value of v was obtained by trial and error, and the best results were obtained for $N = 5$. It should be noted that output layer dimensions (4 $\times$ 4) to (13 $\times$ 13) over (10–120) epochs was also checked but the best results were achieved using $5 \times 5 = 25$ over 20 epochs. For Kohonen mapping, the MOLMAP toolbox, developed by Milano Chemometrics and QSAR research Group, was used [28].

Modeling procedures

Model development with PLS In this approach the partial least squares (PLS) regression was employed to evaluate the structure–activity relationships and genetic algorithm (GA) was used as variable selection method. In the case of MOLMAP approach the set of 25 Kohonen scores (i.e., 5 $\times$ 5 Nodes) over 60 epochs was used as input. In order to

Table 1 Chemical structure, experimental and predicted class of the antimicrobial activity of compounds used in QSAR analysis against *S. aureus* by GA-PLS and CP-ANN

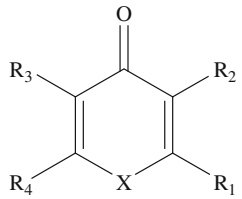

Compd.	X	R_1	R_2	R_3	R4	Experimental MIC (μg/mL)	Activity class of compound	GA-PLS	CP-ANN
1	NH	CH_3	OH	CH_2–R^a	H	64	2	2	2
2	NH	C_2H_5	OH	CH_2–R^a	H	512	3	3	3
3	NH	CH_3	OH	CH_2–$N(CH_3)_2$	H	512	3	3	3
4	NH	C_2H_5	OH	CH_2–$N(CH_3)_2$	H	512	3	3	3
5*	NH	CH_3	OH	CH_2–$N(C_2H_5)_2$	H	512	3	3	3
6	NH	C_2H_5	OH	CH_2–$N(C_2H_5)_2$	H	512	3	3	3
7	N–Ph	CH_3	OH	H	H	128	2	2	2
8*	N–*m*–OH–Ph	CH_3	OH	H	H	512	3	3	3
9	N–C_3H_7	CH_3	OH	H	H	512	3	3	3
10	N–C_4H_9	CH_3	OH	H	H	128	2	2	2
11	O	CH_2Cl	H	OH	H	256	3	3	3
12	O	CH_3	H	OH	H	256	3	3	3
13	O	CH_2OH	OH	H	CH_3	256	3	3	3
14	O	CH_2OH	OCH_2Ph	H	CH_3	256	3	3	3
15	O	CHO	OCH_2Ph	H	CH_3	64	2	2	2
16	O	COOH	OCH_2Ph	H	CH_3	256	3	3	3
17	O	$CONHR^b$	OCH_2Ph	H	CH_3	256	3	3	3
18	O	$CONHR^c$	OCH_2Ph	H	CH_3	256	3	3	3
19*	O	$CONHR^d$	OCH_2Ph	H	CH_3	128	2	3	3
20	O	$CONHR^b$	OH	H	CH_3	64	2	1	3
21	O	$CONHR^c$	OH	H	CH_3	256	3	3	3
22	O	$CONHR^d$	OH	H	CH_3	8	1	1	3
23	O	CH_2OH	H	OCH_2Ph	H	256	3	3	3
24*	O	COOH	H	OCH_2Ph	H	256	3	3	3
25	O	CONHPh	H	OCH_2Ph	H	128	2	2	2
26	N–CH_3	CONHPh	H	OCH_2Ph	H	128	2	2	2
27	N–CH_3	CONHPh	H	OH	H	16	1	1	1
28*	O	CONH–R^e	H	OCH_2Ph	H	128	2	2	2
29	N–CH_3	CONH–R^e	H	OCH_2Ph	H	256	3	3	1
30*	N–CH_3	CONH–R^e	H	OH	H	32	1	1	1
31	O	CH_2OH	H	OH	H	256	3	3	3

[a] Compounds used as prediction set

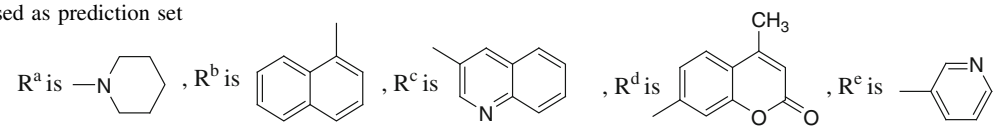

investigate the prediction ability of the models, the data set (n = 31) was divided into two group: calibration set (n = 25) and prediction set (n = 6). Given 25 calibration samples; leave-one out cross-validation procedure was used to find the optimum number of latent variables for each PLS model. GA produces a population of acceptable

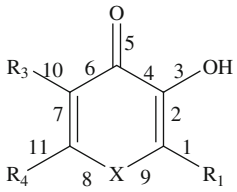

Fig. 1 Common bonds and the number of bonds in the molecules

models in each run. In this work, many different GA-PLS runs were conducted using different initial set of populations (50–250) and therefore a large number of acceptable models were created.

The PLS regression method used was the NIPALS-based algorithm existed in the chemometrics toolbox of MATLAB software (version 7.1 Math work Inc.). Leave-one-out cross-validation procedure was used to obtain the optimum number of factors based on the Haaland and Thomas F-ratio criterion [29].

Model development with CP-ANNs Genetic algorithm (GA) was used for variable selection. Counter-propagation artificial neural networks (CP-ANNs) were used to model the relationship between the MOLMAP descriptors of the compounds and the corresponding MIC values. Four MOLMAP descriptors selected by genetic algorithm were used to train CP-ANNs of size 7×7 nodes over 60 epochs. Leave-one-out (LOO) method was used to predict the class of the compounds. CP-ANNs are very similar to Kohonen maps and are essentially based on the Kohonen approach, but combine characteristics from both supervised and unsupervised learning [30]. CP-ANNs consist of two layers of neurons. The first layer is a Kohonen map, and this is responsible for choosing the winning neuron. It stores information concerning the input data. The second layer; whose neurons have as many weights as the number of classes to be modeled, when dealing with classification issues, have exactly the same number and the same layout of neurons as the Kohonen one. CP-ANN generally is a successful method for modeling classes separated with non-linear boundaries [30].

Chemistry

All chemicals used for the synthesis of the compounds were purchase from Merck or Fluka. Melting points were determined on a Mettler capillary melting point apparatus and were uncorrected. The IR spectra were recorded on a WQF-510 Ratio Recording FT-IR spectrometer as a KBr disc (γ, cm^{-1}). The ^{1}H-NMR spectra (DMSO-d_6) were recorded on a Bruker 400 MHz spectrometer. Chemical shifts (δ) are reported in ppm downfield from the internal standard tetramethylsilane (TMS). The mass spectra were acquired with a Finnigan TSQ-70 mass spectrometer. Electron-impact ionization was performed at an ionizing energy of 70 eV. The synthesis pathway followed for the preparation of the compounds is represented in Scheme 1. The commercially available maltol was chosen as starting compound to design several novel acylhydrazone derivatives. 3-(3-hydroxy-2-methyl-4-oxopyridin-1(4*H*)-yl) benzoic acid (**2**) was prepared by the reaction of maltol (**1**) and 3-aminobenzoic acid in aqueous ethanol at pH 5.0 [31]. Compounds **3** and **4** were prepared according to our recent report [32] as follows. Carboxylic acid **2** was treated in methanol with carbonyl diimidazole (DCI) and dimethyl aminopyridine (DMAP) to furnish the desired methyl 3-(3-hydroxy-2-methyl-4-oxopyridin-1(4*H*)-yl) benzoate (**3**) derivative. Refluxing **3** with hydrazine-hydrate in methanol produced 3-(3-hydroxy-2-methyl-4-oxopyridin-1(4*H*)-yl) benzohydrazide (**4**), which was condensed with an aromatic aldehyde to yield (**5a–o**). Compounds **5p–s** were prepared by the same method and recently reported by this group [32].

General procedure for the synthesis of 3-[3-Hydroxy-2-methyl-4-oxopyridine-1(4*H*)-yl] benzoic acid [aryl (hetaryl) methylene]-hydrazides (**5a–o**).

Equimolar amounts of **4** and appropriate aldehyde (1.00 mmol) in 20 mL ethanol were heated under reflux for 24 h. The obtained precipitate was filtered and recrystallized twice from ethanol/diethyl ether (compounds **5a**, **5e**, **5g**, **5m**, **5p**, **5q**, **5r**, and **5s**). The other compounds (**5b**, **5c**, **5d**, **5f**, **5h**, **5i**, **5j, 5k, 5l, 5n,** and **5o**) were purified by preparative thin layer chromatography using (chloroform/methanol:100/8).

Antimicrobial activity determination

Mueller–Hinton broth at pH 7.0 was used to culture *S. aureus* [33]. The inoculum of microorganism (10^8 c.f.u/mL) was cultured for 16–24 h at 37 °C and prepared to turbidity equivalent to McFarland standard No. 0.5 The final size of inoculum was 1.5×10^4. The test compounds were dissolved in dimethyl sulfoxide (DMSO) (final concentration of 0.5 % v/v) and diluted with culture broth to concentration of 512 μg/mL. Serial two fold dilutions were made in concentration range from 1 to 512 μg/mL in sterile 96-well microplates. 100 μL of each dilution were distributed in 96-well microplates, as well as a sterility control and a growth control (containing culture broth plus DMSO, without antimicrobial substance). 100 μL of a 24 h old inoculum of 10^5 c.f.u/mL was added to each well. Plates were covered and sealed with parafilm and incubated for 24 h at 37 °C. MIC values were defined as the lowest concentration of each tested compound, which completely inhibited microbial growth [34]. Ampicilin and tetracycline were used as standard antibacterial drugs.

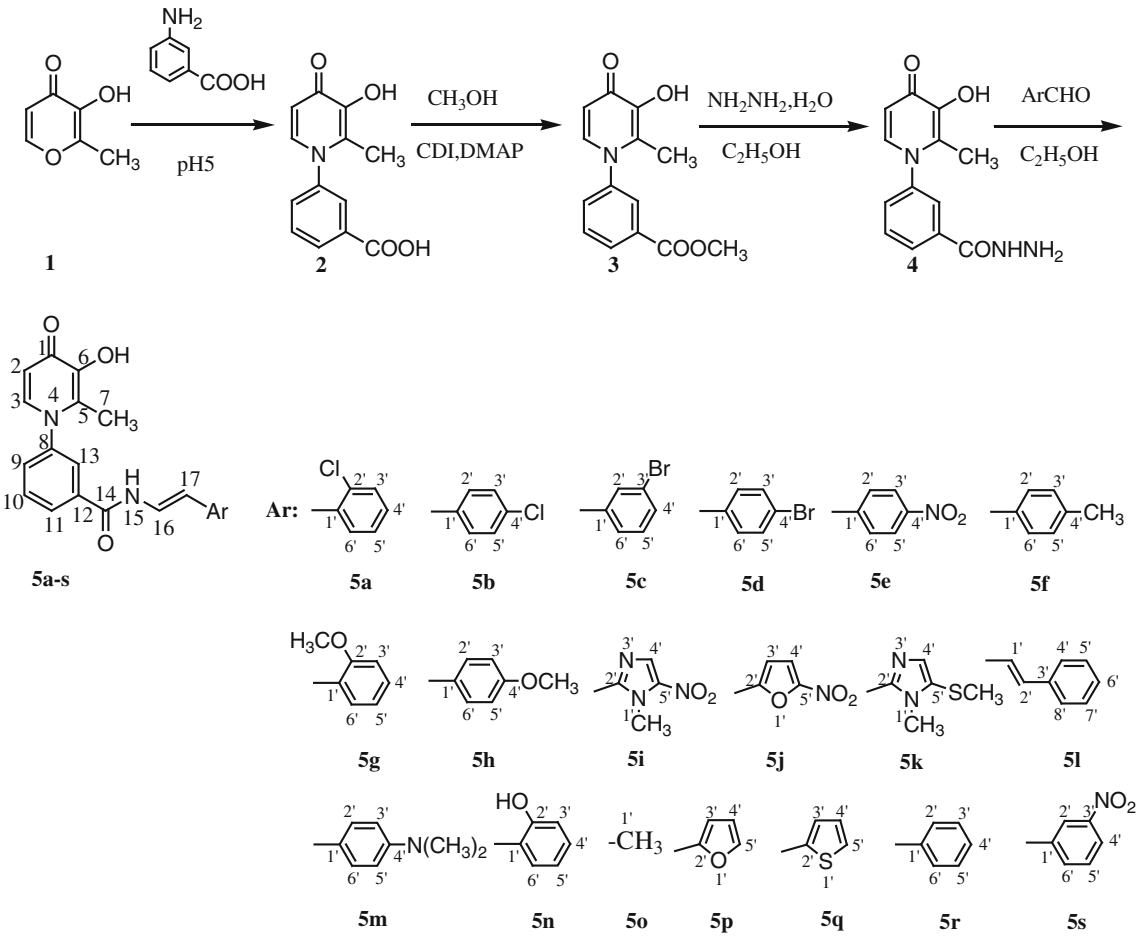

Scheme 1 Synthesis of N-aryl-3-hydroxypyridine-4-ones **5a–s**

Results and discussions

QSAR analysis

Analysis of empirical physicochemical parameters by MOLMAP approach

In the case of MOLMAP analysis, the empirical physicochemical parameters should be arranged in a three-way array in the direction of molecules, bonds and empirical physicochemical parameters. Then, this 3D array should be introduced as input of Kohonen network to obtain the related scores. Here, we investigated different dimensions in the range of (4 × 4) to (13 × 13) over different epochs (20–120) and, in each case; the resulting scores were used as input of GA-PLS model. Best results were obtained by a (5 × 5) over 20 epochs dimension for all data sets. The PLS estimate of the regression coefficients is shown in Figure 2s. The distribution of bonds in the resulted Kohonen map (5 × 5) is represented in Figure 3s. It should be noted that the map contains 25 nodes, which can be numbered sequentially from 1 to 25 so that the nodes of the first row are numbered as N_1–N_5, those of the second row as N_6–N_{12} and so on. The map shows a relatively random distribution of bonds. The scores of this map (25 variables) were used as input of GA-PLS regression. The relative importance of selected neurons for GA-PLS model is shown in Figure 3s.

The resulted GA-PLS models using MOLMAP scores as input variables possessed high prediction ability to determine the activity class of compounds in the calibration set. All molecules in this set (Table 1) were correctly predicted as active, moderately active and inactive as it was experimentally observed. The results are shown in Table 1. The predictive ability of the model was measured by application of 6 external test set molecules. The model also is able to correctly predict the activity class of compounds. Five out of six molecules were correctly predicted while molecule 27 was experimentally active but was predicted to be moderately active by this model. This model was applied for the prediction of the activity class of 302 novel 3-hydroxypyridine-4-one derivatives. The structures of these compounds are depicted in Table 1s. Most of these compounds have not been synthesized and none of them

Table 2 Predicted classes of N-aryl-3-hydroxypyridine-4-ones **5a–s**

No.	GA-PLS	CP-ANN
5a	2	3
5b	2	2
5c	3	3
5d	3	3
5e	1	1
5f	3	2
5g	1	1
5h	2	2
5i	2	2
5j	2	2
5k	2	2
5l	3	3
5m	2	2
5n	2	2
5o	3	3
5p	2	2
5q	2	3
5r	2	2
5s	2	2

have been evaluated for antimicrobial activity yet. The prediction results are shown in Table 2s. The prediction results of N-aryl-3-hydroxypyridine-4-ones **5a–s** are shown in Table 2. Tables 1s, 2s and Figures 2s, 3s are shown in the supplementary materials.

Analysis of MOLMAP descriptors by CP-ANNs approach

GA-PLS method applied a regression-based approach to predict the activity of the studied compounds. The biological activity class of discrete values can also be modeled by classification-based methods. Here CP-ANN was used as a classification method. CP-ANNs were trained to predict the activity class of the compounds on the basis of four MOLMAP descriptors selected by GA. To find optimal CP-ANN settings, several networks were evaluated by changing the number of neurons and training epochs. Settings were then selected on the basis of optimization of a classification parameter, such as error rate, evaluated in cross validation. In Table 3 part of the classification indices calculated by the toolbox (non error rate and error rate) is shown. In Table 4, the other classification indices (specificity, sensitivity, and precision) are shown for all modeled

Table 3 Non-error rate (NER) and error rate (ER) obtained in fitting and cross-validation

	Fitting	Cross-validation
NER	0.83	0.79
ER	0.17	0.21

Table 4 Specificity (SP), sensitivity (Sn), and precision (P) for all the predefined activity classes obtained in cross-validation

Activity class	SP	Sn	P
1	0.97	1	0.94
2	0.91	0.77	0.92
3	0.80	0.93	0.93

activity classes. The top map of the calculated model (7×7 neurons and 60 epochs) is shown in the Fig. 2. In the top map with 49 neurons, each sample is labeled on the basis of the Kohonen weight of variable 1, going from low values (white) to high values (black). Since the model was built with a toroidal boundary condition, each edge of the Kohonen map has to be seen as connected with the opposite ones. It was seen that variable 1 is more influential on the molecules of activity class 2 than the molecules of the class 1 and 3. Therefore, it is possible to inspect each variable on the top map, at the same time. The profile of Kohonen weights of one of the neurons where class 2 molecules are placed is shown in Figure 4s. It was seen that molecules in this class are characterized by having high values of variable 1 and 4, low values of variable 2, and extremely low values of variable 3. It is not possible to have a comprehensive insight into the relationships between variables and molecules, since we can only plot the weights of one variable at a time for all the neurons (Fig. 2) or, on the contrary, the variable profile of one neuron simultaneously (Figure 4s). The weights of Kohonen layer are arranged as a data matrix **W** with 49 rows and 4 columns, as explained before, and PCA was calculated. In Figs. 3 and 4 the score and loading plots of the first two components (explaining together 83 % of the total

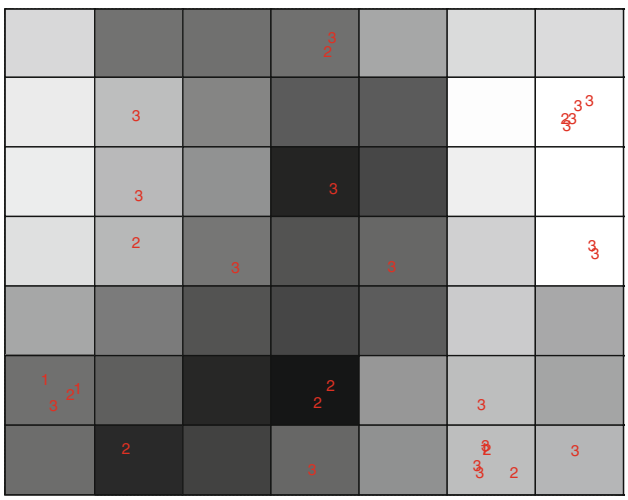

Fig. 2 Kohonen top map with toroidal boundary condition, each molecule is labeled on the basis of its class; neurons are *colored* on the basis of the weight of variable 1

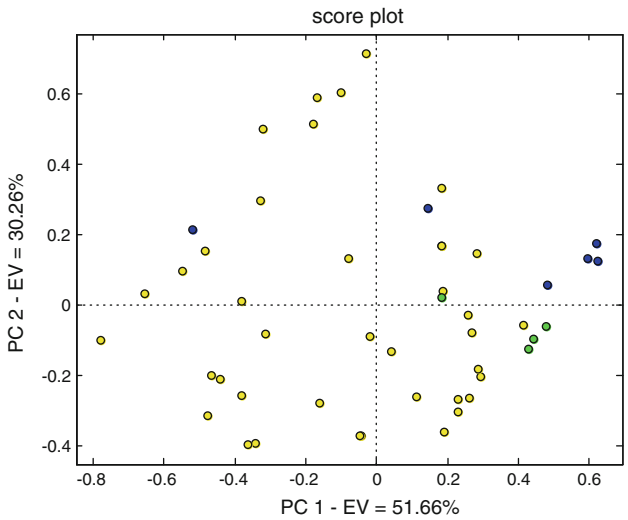

Fig. 3 Score plot of the first two principal components calculated on the Kohonen weights. Each neuron is *colored* on the basis of the output weight of each activity class. Active, partially active, and inactive neurons are in *green*, *blue* and *yellow* color, respectively

information) are shown, respectively. In the score plot of Figs. 3, each point represents a neuron of the previous CP-ANN model. Each neuron is colored on the basis of the output weight of each activity class (three classes). For example the neurons assigned to class 2 are all clustered and placed at the left side of the score plot. Variables 1 and 4 are placed at the left side of the loading plot and thus are directly correlated with class 2; on the contrary, variable 3 has the largest positive loadings in the first component and the molecules of class 2 will be characterized by small value of this variable. The same conclusion could be made by analyzing the single profile of Figure 4s. Figure 5

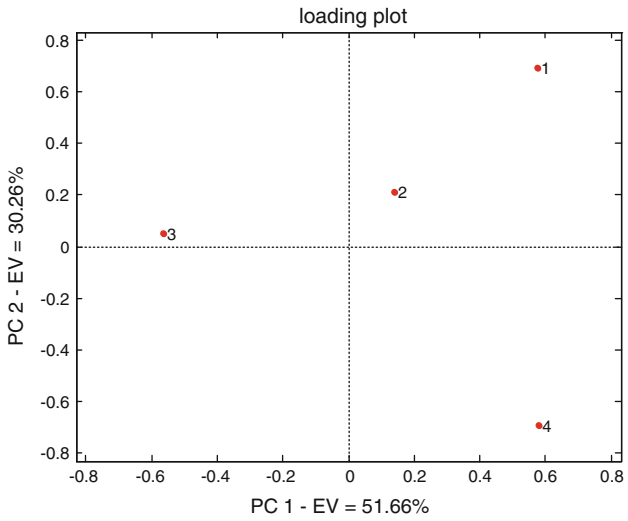

Fig. 4 Loading plot of the first two principal components calculated on the Kohonen weights. Each variable is labeled with its identification *number*

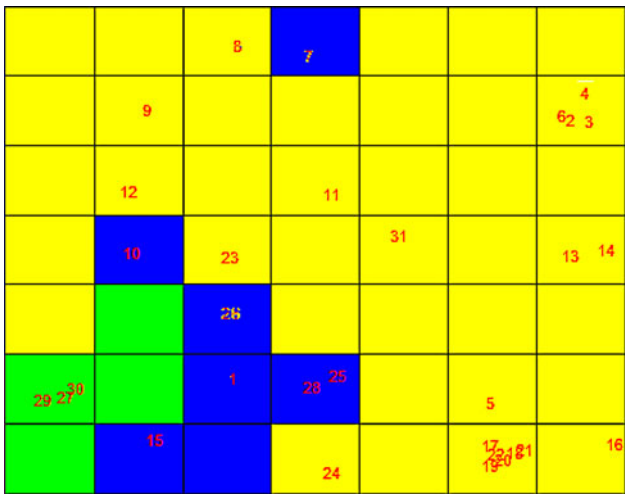

Fig. 5 Representation of the CP-ANN output layer, with neurons predicted as active, partially active, and inactive (*green*, *blue* and *yellow* color, respectively)

highlights the relationships between structural features and the class of compounds. Inspection of a CP-ANN trained with all molecules (Fig. 5) revealed that structurally similar molecules were mapped together in one neuron or as a cluster of neurons. In this figure, the neurons with a low output (inactive molecules) are colored in yellow and neurons corresponding to active and moderately active molecules are colored in green and blue, respectively. Molecules 27, 29 and 30 which were predicted to be potent appeared in a single neuron at the bottom left. Two of these three molecules were experimentally observed to be active (the first class) and one inactive (molecule 29 in the third class). Molecules 1, 7, 10, 15, 25, 26 and 28 were clustered to each other at the mid, bottom and top of the CP-ANN surface in Fig. 5. All of these compounds were correctly predicted to be moderately active.

Twenty-one molecules predicted inactive were clustered into yellow neurons. Eighteen out of twenty-one molecules were experimentally observed to be inactive whereas two molecules were identified as moderately active (molecules 19 and 20) and one as active (molecule 22). Figure 4s is shown in the supplementary materials.

Proposing new compounds

Based on the developed QSAR models by GA-PLS and CP-ANN, and considering the structural similarities with the studied compounds, 302 more compounds, most of them have not been previously synthesized, were proposed and their antimicrobial activities were predicted. The results are shown in Table 2s and Table 2.

To evaluate the predictability and accuracy of the obtained QSAR models, 19 compounds belonging to all three activity classes were selected among the 302

compounds. The proposed compounds were synthesized and their antimicrobial activity was evaluated against *S. aureus*. Comparing the experimental results (as MIC) for anti *S. aureus* activity and the predicted activity classes, the accuracy of the obtained models can be judged. The collected results in Table 2 disclose this fact that seventeen out of the nineteen synthesized molecules were correctly predicted by GA-PLS model according to antimicrobial evaluation method. Two molecules (**5f** and **5h**) proved to be experimentally moderately active and active, respectively but were predicted to be inactive and moderately active by this model, respectively.

The CP-ANN based prediction was correct for sixteen out of the nineteen synthesized molecules. Three molecules (**5a**, **5h** and **5q**) were moderately active and active based on the antimicrobial assays but they were introduced as members of inactive, moderately active and inactive class of compounds according to CP-ANN model.

Chemistry

Formation of the desired compounds was confirmed with FT-IR, ^{1}H-NMR and Mass spectra. All spectral data are provided below. Carbon atoms are numbered sequentially to facilitate the assignment of protons in ^{1}H-NMR spectra (Scheme 1). The hydrazone N=CH- and -NH-signals appeared as two singlets at 8.09–9.00 and 11.59–12.35, respectively. H_2 signal was seen among a group of signals belonging to the aromatic protons. H_3 was observed in all molecules as a doublet (J constant = 8.00 Hz) at 6.22–7.20. Singlet signal belonging C_5–CH_3 hydrogens was found in the range of 1.96–2.06. A broad singlet for C_4–OH appeared at 3.40–3.80. In all Mass spectra a fragment with the molecular weight of about 199 was detected. This fragment can be attributed to $C_{12}H_9NO_2$ in which the acylhydrazone moiety is cleaved and the hydroxyl proton on the 3-hydroxyopyridin-4-one scaffold is gone.

*3-[3-Hyroxy-2-methy-4-oxopyridin-1(4H)-yl] benzoic acid (2-chloro-phenyl methylene)-hydrazide (**5a**)* 118.87 mg (82 %) compound was obtained as light pink crystals, m.p. 158–159 °C; FT-IR (KBr Disc) ν/cm^{-1}: 3130–3300 (broad, NH and OH), 3064 (CH, aromatic), 2980 (CH, aliphatic), 1684 (C=O, ketone), 1628 (C=O, acylhydrazone), 1577 (shouldered, C=N, C=C), 1489 (C=C aromatic); ^{1}H-NMR (DMSO-d_6, 400 MHz): (δppm) 12.14 (s, 1H, NH), 8.84 (1H, N=CH_{17}), 8.09 (bs, 1H, H_{10}), 7.98–8.06 (m, 2H, H_{13}, $H_{3'}$), 7.70–7.76 (m, 2H, H_9, H_{11}), 7.65 (d, J = 7.20 Hz, 1H, H_2), 7.54 (d, 1H, $H_{6'}$), 7.42–7.48 (m, 2H, $H_{4'}$, $H_{5'}$), 6.27 (d, J = 7.20 Hz, 1H, H_3), 3.42 (bs, 1H, OH), 2.00 (s, 3H, C_5–CH_3). MS (EI): m/z = 199.1 [$M^{+\cdot}$–CONHN=CHC_6H_4Cl, 100 %], 381.2 [$M^{+\cdot}$ ($^{35.5}$Cl), 96 %], 383.2 [$M^{+\cdot}$ ($^{37.5}$Cl), 37 %].

*3-[3-Hyroxy-2-methy-4-oxopyridin-1(4H)-yl] benzoic acid (4-chloro-phenyl methylene)-hydrazide (**5b**)* 118.87 mg (82 %) compound was obtained as a light pink crystals, m.p. 219–220 °C; FT-IR (KBr Disc) ν/cm^{-1}: 3150–3300 (broad, NH and OH), 3064 (CH, aromatic), 2925 (CH, aliphatic), 1668 (C=O, ketone), 1628 (C=O, acylhydrazone), 1577 (shouldered C=C, C=N), 1491 (C=C aromatic); ^{1}H-NMR (DMSO-d_6, 400 MHz): (δppm) 12.00 (s, 1H, NH), 8.42 (1H, N=CH_{17}), 8.09 (bs, 1H, H_{10}), 7.98 (bs, 1H, H_{13}), 7.70–7.80 (m, 4H, H_9, H_{11}, $H_{3'}$, $H_{5'}$), 7.62 (m, 1H, H_2), 7.52 (d, J = 8.00 Hz, 2H, $H_{2'}$, $H_{6'}$), 6.23 (m, 1H, H_3), 3.41(bs, 1H, OH), 1.99 (s, 3H,C_5–CH_3). MS (EI): m/z = 199.2 [$M^{+\cdot}$–CONHN=CHC_6H_4Cl, 80 %], 381.2 [$M^{+\cdot}$ ($^{35.5}$Cl), 100 %], 383.2 [$M^{+\cdot}$ ($^{37.5}$Cl), 38 %].

3-[3-Hyroxy-2-methy-4-oxopyridin-1(4H)-yl] benzoic acid (3-bromo-phenyl methylene)-hydrazide (**5c**) 121.69 mg (75 %) compound was obtained as a light pink crystals, m.p. 258–259 °C; FT-IR (KBr Disc) ν/cm^{-1}: 3433 (NH), 3359 (OH), 3062 (CH, aromatic), 2970 (CH, aliphatic), 1660 (C=O, ketone), 1628 (C=O, acylhydrazone), 1572 (shouldered, C=N, C=C), 1495 (C=C aromatic); ^{1}H-NMR (DMSO-d_6, 400 MHz): (δppm) 12.06 (s, 1H, NH), 8.40 (1H, N=CH_{17}), 8.06 (s, 1H, H_{10}), 7.94–7.98 (m, 2H, H_{13}, $H_{2'}$), 7.61–7.77 (m, 5H, H_2, H_9, H_{11}, $H_{4'}$, $H_{6'}$), 7.43 (t, 1H, $H_{5'}$), 6.25 (d, J = 8.00 Hz, 1H, H_3), 3.42 (s, 1H, OH), 2.00 (s, 3H,C_5–CH_3). MS (EI): m/z = 199.1 [$M^{+\cdot}$–CONHN=CHC_6H_4Br, 100 %], 427.2 [$M^{+\cdot}$ (^{79}Br)$^{\cdot}$, 66 %], 429.2 [$M^{+\cdot}$ (^{81}Br)$^{\cdot}$, 66 %].

*3-[3-Hyroxy-2-methy-4-oxopyridin-1(4H)-yl] benzoic acid (4-bromo-phenyl methylene)-hydrazide (**5d**)* 113.58 mg (70 %) compound was obtained as a light pink crystals, m.p. 174–175 °C; FT-IR (KBr Disc) ν/cm^{-1}: 3100–3250 (broad, NH and OH), 3003 (CH, aromatic), 2925 (CH, Aliphatic), 1668 (C=O, ketone), 1630 (C=O, acylhydrazone), 1570 (shouldered, C=N, C=C), 1487 (C=C aromatic); ^{1}H-NMR (DMSO-d_6, 400 MHz): (δppm) 11.98 (s, 1H, NH), 8.40 (1H, N=CH_{17}), 8.06 (bs, 1H, H_{10}), 7.96 (bs,1H, H_{13}), 7.62–7.78 (m, 7H, H_2, H_9, H_{11}, $H_{2'}$, $H_{3'}$, $H_{5'}$, $H_{6'}$), 6.25 (bs, 1H, H_3), 3.42 (bs, 1H, OH), 1.98 (s, 3H,C_5–CH_3). MS (EI): m/z = 199.1 [$M^{+\cdot}$–CONHN=CHC_6H_4Br, 100 %], 427.2 [$M^{+\cdot}$ (^{79}Br), 83 %], 429.2 [$M^{+\cdot}$ (^{81}Br), 83 %].

*3-[3-Hyroxy-2-methy-4-oxopyridin-1(4H)-yl] benzoic acid (4-nitro-phenyl methylene)-hydrazide (**5e**)* 119.16 mg (80 %) compound was obtained as a light brown crystals, m.p. 290–291 °C; FT-IR (KBr Disc) ν/cm^{-1}: 3329 (NH), 3211(OH), 3064 (CH, aromatic), 2925 (CH, aliphatic), 1672 (C=O, ketone), 1630 (C=O, acylhydrazone), 1570 (shouldered, C=N, C=C), 1497 (C=C aromatic); ^{1}H-NMR (DMSO-d_6, 400 MHz): (δppm) 12.21 (s, 1H, NH), 8.54 (1H, N=CH_{17}), 8.31 (d, J = 8.00 Hz, 2H, $H_{3'}$, $H_{5'}$), 8.09 (s,

1H, H_{10}), 8.00 (d, 3H, H_9, H_{11}, H_{13}), 7.72–7.76 (d, 2H, $H_{2'}$, $H_{6'}$), 7.65 (d, J = 7.78 Hz, 1H, H_2), 6.27 (d, J = 7.78 Hz, 1H, H_3), 3.43 (bs, 1H, OH), 2.00 (s, 3H, C_5–CH_3). MS (EI): m/z = 199.1 [$M^{+\cdot}$–CONHN=$CHC_6H_4NO_2$, 75 %], 392.2 [$M^{+\cdot}$, 100 %].

*3-[3-Hyroxy-2-methy-4-oxopyridin-1(4H)-yl] benzoic acid (4-methyl-phenyl methylene)-hydrazide (**5f**)* 102.88 mg (75 %) compound was obtained as a light pink crystals, m.p. 244–245 °C; FT-IR (KBr Disc) ν/cm^{-1}: 3250–3300 (broad, NH and OH), 3075 (CH, aromatic), 2922 (CH, aliphatic), 1682 (C=O, ketone), 1630 (C=O, acylhydrazone), 1570 (shouldered, C=N, C=C), 1483 (C=C, aromatic); ^{1}H-NMR (DMSO-d_6, 400 MHz): (δppm) 11.85 (s, 1H, NH), 8.39 (1H, N=CH_{17}), 8.05 (bs, 1H, H_{10}), 7.96 (bs, 1H, H_{13}), 7.71 (bs, 2H, H_9, H_{11}), 7.60–7.66 (m, 3H, H_2, $H_{3'}$, $H_{5'}$), 7.28 (d, 2H, $H_{2'}$, $H_{6'}$), 6.25 (d, J = 8.00 Hz, 1H, H_3), 3.42 (bs, 1H, OH), 2.34 (s, 3H, $C_{4'}$–CH_3), 1.99 (s, 3H,C_5–CH_3). MS (EI): m/z = 199.1 [$M^{+\cdot}$–CONHN=$CHC_6H_4CH_3$, 75 %], 361.2 [$M^{+\cdot}$, 100 %].

*3-[3-Hyroxy-2-methy-4-oxopyridin-1(4H)-yl] benzoic acid (2-methoxy-phenyl methylene)-hydrazide (**5g**)* 117.47 mg (82 %) compound was obtained as a white crystals, m.p. 187–188 °C; FT-IR (KBr Disc) ν/cm^{-1}: 3413 (NH), 3209 (OH), 3070 (CH, aromatic), 2927 (CH, aliphatic), 1653 (C=O, ketone), 1620 (C=O, acylhydrazone), 1599 (C=C, aromatic), 1572 (shouldered, C=N, C=C), 1483 (C=C, aromatic); ^{1}H-NMR (DMSO-d_6, 400 MHz): (δppm) 11.89 (s, 1H, NH), 8.79 (1H, N = CH_{17}), 8.07 (s, 1H, H_{10}), 7.98 (s, 1H, H_{13}), 7.88 (d, J = 8.00 Hz, 1H, $H_{6'}$), 7.73–7.69 (m, 2H, H_9, H_{11}), 7.59–7.62 (bs, 1H, H_2), 7.43 (t, J = 8.00 Hz, 1H, $H_{5'}$), 7.12 (d, J = 8.00 Hz, 1H, $H_{3'}$), 7.03 (t, 1H, $H_{4'}$), 6.24 (d, J = 7.78 Hz, 1H, H_3), 3.37 (bs, 1H, OH), 3.86 (s, 3H, OCH_3), 2.00 (s, 3H,C_5–CH_3). MS (EI): m/z = 199.2 [$M^{+\cdot}$–CONHN=$CHC_6H_4OCH_3$, 90 %], 377.3 [$M^{+\cdot}$, 100 %].

*3-[3-Hyroxy-2-methy-4-oxopyridin-1(4H)-yl] benzoic acid (4-methoxy-phenyl methylene)-hydrazide (**5h**)* 114.60 mg (80 %) compound was obtained as a white crystals, m.p. 281–282 °C; FT-IR (KBr Disc) ν/cm^{-1}: 3200–3300 (broad, NH and OH), 3068 (CH, aromatic), 2920 (CH, aliphatic), 1670 (C=O, ketone), 1628 (C=O, acylhydrazone), 1608 (C=C, aromatic), 1572 (shouldered, C=N, C=C), 1495 (C=C, aromatic); ^{1}H-NMR (DMSO-d_6, 400 MHz): (δppm) 11.79 (s, 1H, NH), 8.38 (1H, N = CH_{17}), 8.05 (bs, 1H, H_{10}), 7.96 (bs, 1H, H_{13}), 7.65–7.73 (m, 4H, H_9, H_{11}, $H_{2'}$, $_{6'}$), 7.63 (d, J = 7.2 Hz, 1H, H_2), 7.02 (d, J = 8.00 Hz, 2H, $H_{3'}$, $H_{5'}$), 6.24 (d, J = 7.2 Hz, 1H, H_3), 3.80 (s, 3H, OCH_3), 1.99 (s, 3H, C_5–CH_3). MS (EI): m/z = 199.2 [$M^{+\cdot}$–CONHN=$CHC_6H_4OCH_3$, 45 %], 377.3 [$M^{+\cdot}$, 100 %].

*3-[3-Hydroxy-2-methyl-4-oxopyridin-1(4H)-yl] benzoic acid [(1-methyl-5-nitro-1H-imidazol-2-yl)methylene]- hydrazide (**5i**)* 109.85 mg (73 %) compound was obtained as a yellow crystals, m.p. 284–285 °C; FT-IR (KBr Disc) ν/cm^{-1}: 3100–3250 (broad, NH and OH), 3050 (CH, aromatic), 2964 (CH, aliphatic), 1684 (C=O, ketone), 1630 (C=O, acylhydrazone), 1579 (shouldered, C=N, C=C), 1487 (C=C Aromatic); ^{1}H-NMR (DMSO-d_6, 400 MHz): (δppm) 12.27 (s, 1H, NH), 8.45 (1H, N = CH_{17}), 8.22 (s, 1H, $H_{4'}$), 8.08 (bs, 1H, H_{10}), 7.97 (bs, 1H, H_{13}), 7.73–7.78 (m, 2H, H_9, H_{11}), 7.63 (d, 1H, H_2), 6.24 (d, 1H, H_3), 4.28 (s, 3H, N–CH_3), 3.39 (bs, 1H, OH), 1.99 (s, 3H, C_5–CH_3). MS (EI): m/z = 199.1 [$M^{+\cdot}$–CONHN=$CHC_3H_4N_3O_2$, 100 %], 396.2 [$M^{+\cdot}$, 33 %].

*3-[Hyroxy-2-methy-4-oxopyridin-1(4H)-yl] benzoic acid [(5-nitrofuran-2-yl) methylene]-hydrazide (**5j**)* 113.22 mg (78 %) compound was obtained as a yellow crystals, m.p. 260–261 °C; FT-IR (KBr Disc) ν/cm^{-1}: 3100–3400 (broad, NH and OH), 3066 (CH, aromatic), 2990 (CH, aliphatic), 1695 (C=O, ketone), 1635 (C=O, acylhydrazone), 1564 (shouldered, C=N, C=C), 1477 (C=C aromatic); ^{1}H-NMR (DMSO-d_6, 400 MHz): (δppm) 12.35 (s, 1H, NH), 8.40 (1H, N = CH_{17}), 8.09 (bs, 1H, H_{10}), 7.99 (s, 1H, H_{13}), 7.80 (d, 1H, $H_{4'}$), 7.75–7.78 (m, 2H, H_9, H_{11}), 7.70 (d, J = 7.78 Hz, 1H, H_2), 7.30 (bs, 1H, $H_{3'}$), 6.34 (d, J = 7.78 Hz, 1H, H_3), 3.40 (bs, 1H, OH), 2.01 (s, 3H, C_5–CH_3). MS (EI): m/z = 199.1 [$M^{+\cdot}$–CONHN=$CHC_4H_2NO_3$, 100 %], 382.2 [$M^{+\cdot}$, 33 %].

*3-[3-Hydroxy-2-methyl-4-oxopyridin-1(4H)-yl] benzoic acid [(1-methyl-2-(methylthio)-1H-imidazol-5-yl)methylene]-hydrazide (**5k**)* 98.05 mg (65 %) compound was obtained as a yellow crystals, m.p. 278–279 °C; FT-IR (KBr Disc) ν/cm^{-1}: 3100–3300 (broad, NH and OH), 3060 (CH, aromatic), 2933 (CH, aliphatic), 1674 (C=O, ketone), 1628 (C=O, acylhydrazone), 1574 (shouldered, C=N, C=C), 1485 (C=C aromatic); ^{1}H-NMR (DMSO-d_6, 400 MHz): (δppm) 11.76 (s, 1H, NH), 8.33 (1H, N = CH_{17}), 8.03 (bs, 1H, H_{10}), 7.93 (s,1H, H_{13}), 7.68–7.72 (m, 2H, H_9, H_{11}), 7.63 (d, J = 8.00 Hz, 1H, H_2), 7.41 (s, 1H, $H_{4'}$), 6.24 (d, J = 8.00 Hz, 1H, H_3), 3.83 (s, 3H, N–CH_3), 3.42 (bs, 1H, OH), 2.59 (s, 3H, S–CH_3), 1.99 (s, 3H, C_5–CH_3). MS (EI): m/z = 199.1 [$M^{+\cdot}$–CONHN=$CHC_4H_7N_2S$, 100 %], 397.2 [$M^{+\cdot}$, 96 %].

*3-[3-Hydroxy-2-methyl-4-oxopyridin-1(4H)-yl benzoic acid (Phenylvinyl) -hydrazide. (**5l**)* 110.55 mg (78 %) compound was obtained as a yellow to white crystals, m.p. 189–190 °C; FT-IR (KBr Disc) ν/cm^{-1}: 3200–3300 (broad, NH and OH), 3037 (CH, aromatic), 2935 (CH, aliphatic), 1674 (C=O, ketone), 1626 (C=O, acylhydrazone), 1562 (shouldered, C=N, C=C), 1479 (C=C aromatic); ^{1}H-NMR (DMSO-d_6, 400 MHz): (δppm) 11.81 (s, 1H, NH), 8.30 (1H, N = CH_{17}), 8.22 (bs, 1H, H_{10}), 7.95 (bs, 1H, H_{13}), 7.68–7.73(m, 2H, H_9, H_{11}), 7.60–7.66 (m, 3H, H_2, $H_{4'}$, H $_{8'}$), 7.31–7.40 (m, 3H, $H_{5'}$, $H_{6'}$, $H_{7'}$), 7.04–7.10 (m, 2H,

$H_{1'}$, $H_{2'}$), 6.24 (m, 1H, H_3), 3.56 (bs, 1H, OH), 1.99 (s, 3H, C_5–CH_3). MS (EI): m/z = 199.2 [$M^{+\cdot}$–CONHN=CHC_8H_7, 60 %], 373.3 [$M^{+\cdot}$, 100 %].

*3-[3-Hyroxy-2-methy-4-oxopyridin-1(4H)-yl]) benzoic acid (4-dimethylamino- phenyl methylene)-hydrazide (**5m**)* 121.52 mg (82 %) compound was obtained as a yellow crystals, m.p. 201–202 °C; FT-IR:(KBr Disc) FT IR: (KBr Disc) ν/cm^{-1}: 3100–3500 (broad, NH and OH), 3072 (CH, aromatic), 2922 (CH, aliphatic), 1653 (C=O, ketone), 1630 (C=O, acylhydrazide), 1597 (C=N), 1576 (C=C), 1483 (C=C aromatic); ^{1}H-NMR (DMSO-d_6, 400 MHz): (δppm) 11.61 (s, 1H, NH), 8.28 (1H, N=CH_{17}), 8.04 (bs, 1H, H_{10}), 7.94 (bs, 1H, H_{13}), 7.68–7.72 (m, 2H, H_9, H_{11}), 7.62 (d, J = 8.00 Hz, 1H, H_2), 7.53 (d, J = 8.00 Hz, 2H, $H_{3'}$, $H_{5'}$), 6.77 (d, J = 8.00 Hz, 2H, $H_{2'}$, $H_{6'}$), 6.23 (d, J = 8.00 Hz, 1H, H_3), 3.42 (bs, 1H, OH), 2.97 (s, 6H, N–CH_3), 1.99 (s, 3H,C_5–CH_3). MS (EI): m/z = 199.1 [$M^{+\cdot}$–$CONHN=CHC_8H_{10}N$, 25 %], 375.3 [$M^{+\cdot}$–CH3, 100 %], 390.3 [$M^{+\cdot}$, 100 %].

*3-[3-Hydroxy-2-methyl-4-oxopyridin-1(4H)-yl] benzoic acid (2-hydroxy-phenyl methylene)-hydrazide (**5n**)* 93.79 mg (68 %) compound was obtained as a yellow to white crystals, m.p. 284–285 °C; FT-IR (KBr Disc) 3100–3300 (broad, NH and OH), 3064 (CH, aromatic), 2925 (CH, aliphatic), 1670 (C=O, ketone), 1628 (C=O, acylhydrazide), 1570 (shouldered, C=N, C=C), 1493(C=C aromatic); ^{1}H-NMR (DMSO-d_6, 400 MHz): (δppm) 12.13 (s, 1H, NH), 11.12 (bs, 1H, $C_{2'}$–OH), 9.00 (1H, N = CH_{17}), 8.64(bs, 1H, H_{10}), 8.13 (bs,1H, $H_{6'}$), 7.99 (s 1H, H_{13}), 7.54–7.78 (m, 4H, H_2, H_9, H_{11}, $H_{3'}$), 7.39 (t, 1H, $H_{4'}$), 7.30 (t, 1H, $H_{5'}$), 6.25 (d, 1H, H_3), 3.42 (bs, 1H, OH), 1.99 (s, 3H,C_5–CH_3). MS (EI): m/z = 199.1 [$M^{+\cdot}$–$CONHN=CHC_6H_4OH$, 67 %], 227.1 [$M^{+\cdot}$ - $NHN=CHC_6H_4OH$, 100 %], 363.1 [$M^{+\cdot}$, 13 %].

*3-[3-Hyroxy-2-methy-4-oxopyridin-1(4H)-yl] benzoic acid ethylidene-hydrazide (**5o**)]* 82.52 mg (75 %) compound was obtained as a white crystals, m.p. 223–224 °C; FT-IR (KBr Disc) ν/cm^{-1}: 3120–3300 (broad,NH and OH), 3062 (CH, aromatic), 2927 (CH, aliphatic), 1670 (C=O, ketone), 1631 (C=O, acylhydrazide), 1564 (shouldered, C=N, C=C), 1485 (C=C aromatic); ^{1}H-NMR (DMSO-d_6, 400 MHz): (δppm) 11.59 (s, 1H, NH), 8.00–8.09 (m, 2H, N = CH_{17}, H_{10}), 7.90 (bs, 1H, H_{13}), 7.68–7.78 (bs, 2H, H_9, H_{11}), 7.60 (d, 1H, H_2), 6.22 (d, 1H, H_3), 3.49 (bs, 1H, OH), 1.97 (s, 3H, C_5–CH_3), 1.86 (s, 3H, $H_{1'}$). MS (EI): m/z = 199.1 [$M^{+\cdot}$–$CONHN=CHCH_3$, 100 %], 285.1 [$M^{+\cdot}$, 7 %].

*3-[3-Hydroxy-2-methyl-4-oxopyridine-1(4H)-yl] benzoic acid [(furan-2-yl) methylene]-hydrazide (**5p**)*

*3-[3-Hydroxy-2-methyl-4-oxopyridine-1(4H)-yl] benzoic acid [(thiophene-2-yl) methylene]-hydrazide (**5q**)*

*3-[3-Hydroxy-2-methyl-4-oxopyridin-1(4H)-yl] benzoic acid-phenylmethylene-hydrazide (**5r**)*

*3-[3-Hydroxy-2-methyl-4-oxopyridin-1(4H)-yl] benzoic acid (3-nitro-phenyl methylen)-hydrazide (**5s**)* Spectral data for the compounds **5p–s** are described elsewhere [32].

Antimicrobial activity

Minimum inhibitory concentrations (MICs) were determined by microdilution method. *S. aureus* was obtained from the Persian type culture collection (PTCC), Tehran, Iran (PTCC 1112). Mueller–Hinton agar was used to culture this microorganism for 24 h at 37 °C. The antibacterial activity data are given in Table 5.

Significant antibacterial activity was observed in some compounds against *S. aureus*. Compounds **5e**, **5g** and **5h** inhibited the growth of this microorganism at 32 μg/mL. Compounds **5a**, **5b**, **5k**, **5n**, **5p**, **5r**, **5s** showed good inhibitory activity (64 μg/mL) against its growth. It is generally accepted that iron chelators inhibit microbial growth by reducing iron absorption by microorganism.

Table 5 In vitro antibacterial activity (MIC values, μg mL^{-1}) of different 3-hydroxypyridine-4-one derivatives

Compound	MIC (μg mL^{-1})
5a	64
5b	64
5c	256
5d	256
5e	32
5f	128
5g	32
5h	32
5i	128
5j	128
5k	64
5l	256
5m	128
5n	64
5o	256
5p	64
5q	128
5r	64
5s	64
Ampicillin	256
Tetracycline	64

MIC (μg/mL) = minimum inhibitory concentration, i.e., the lowest concentration to completely inhibit bacterial growth

Ampicillin, Tetracycline: standard drug for bacteria

Conclusion

QSAR models allow medicinal chemists to predict the biological activities of untested and even not prepared compounds. Using traditional techniques, it may take months to synthesize a new compound for biological assays. Application of computational techniques for designing biologically active novel compounds reduces experimental research cost and saves a lot of time. Search for new antimicrobial agents with novel modes of action represents a major target in anti infective chemotherapy. The reason is the increasing number of pathogenic bacteria and fungi that are resistant to therapeutic agents. 3-Hydroxypyridine-4-one derivatives have shown good inhibitory activity against bacterial strains such as *S. aureus*. In this work we reported the application of MOLMAP descriptors based on empirical physicochemical properties with GA-PLS and CP-ANN methods to predict some novel 3-hydroxypyridine-4-one derivatives with improved antibacterial activity against this microorganism. A large collection of 302 novel derivatives of this chemical scaffold was selected for this purpose, which the activity class of these compounds was determined using the two QSAR models. To evaluate the predictability and accuracy of the obtained models, nineteen compounds belonging to all three activity classes were prepared and the anti *S. aureus* activity of them was determined. Comparing the experimental results (as MICs) and the predicted activity classes revealed the accuracy of the GA-PLS and CP-ANN models.

In sum, it seems that the MOLMAP approach is a powerful and reliable method to assist medicinal chemists for a rational design of successful bioactive agents.

References

1. Arredondo M, Núñez MT (2005) Iron and copper metabolism. Mol Asp Med 26:313–327
2. Skaar EP, Gaspar A, Schneewind O (2006) Bacillus anthracis IsdG, a heme-degrading monooxygenase. J Bacteriol 188: 1071–1080
3. Hider R, Kong X (2010) Chemistry and biology of siderophores. Nat Prod Rep 27:637–657
4. Aytemir M, Erol D, Hider R, Ozalp M (2003) Synthesis and evaluation of antimicrobial activity of new 3-hydroxy-6-methyl-4-oxo-4*H*-pyran-2-carboxamide derivatives. Turk J Chem 27: 757–764
5. Aytemir M, Hider M, Erol D, Ozalp M, Ekizoglu M (2003) Synthesis of new antimicrobial agents; amide derivatives of pyranones and pyridinones. Turk J Chem 27:445–452
6. Qiu D, Huang Z, Zhou T, Shen C, Hider R (2011) In vitro inhibition of bacterial growth by iron chelators. FEMS Microbiol Lett 314:107–111
7. Dehkordi L, Liu Z, Hider R (2008) Basic 3-hydroxypyridin-4-ones: potential antimalarial agents. Eur J Med Chem 43: 1035–1047
8. Kotani T, Ichimoto I, TatsumI C, Fujita T (1975) Structure-activity study of bacteriostatic kojic acid analogs. Agric Biol Chem 39:1311–1317
9. Kotani T, Ichimoto I, Tatsumi C, Fujita T (1976) Bacteriostatic activities and metal chelation of kojic acid analogs. Agric Biol Chem 40:765–770
10. Feng M, van der Does L, Bantjes A (1993) Iron (III)-chelating resins. 3. Synthesis, iron (III)-chelating properties, and in vitro antibacterial activity of compounds containing 3-hydroxy-2-methyl-4 (1*H*)-pyridinone ligands. J Med Chem 36:2822–2827
11. Fassihi A, Abedi D, Saghaie L, Sabet R, Fazeli H, Bostaki Gh, Deilami O, Sadinpour H (2009) Synthesis, antimicrobial evaluation and QSAR study of some 3-hydroxypyridine-4-one and 3-hydroxypyran-4-one derivatives. Eur J Med Chem 44:2145–2157
12. Hansch C, Hoekman D, Gao H (1996) Comparative QSAR: toward a deeper understanding of chemicobiological interactions. Chem Rev 96:1045–1075
13. Horvath D, Mao B (2003) Neighborhood behavior. Fuzzy molecular descriptors and their influence on the relationship between structural similarity and property similarity. QSAR Comb Sci 22:498–509
14. Putta S, Eksterowicz J, Lemmen C, Stanton R (2003) A novel subshape molecular descriptor. J Chem Inf Comput Sci 43: 1623–1635
15. Ballabio D, Consonni V, Todeschini R (2007) Classification of multiway analytical data based on MOLMAP approach. Anal Chim Acta 605:134–146
16. Zhang Q, Aires-de-Sousa J (2007) Random forest prediction of mutagenicity from empirical physicochemical descriptors. J Chem Inf Model 47:1–8
17. Gupta S, Matthew S, Abreu P, Aires-de-Sousa J (2006) QSAR analysis of phenolic antioxidants using MOLMAP descriptors of local properties. Bioorg Med Chem 14:1199–1206
18. Zupan J, Gasteiger J (1999) Neural networks in chemistry and drug design, 2nd edn. Wiley-VCH, Weinheim
19. Simon V, Gasteiger J, Zupan J (1993) A combined application of 2 different neural-network types for the prediction of chemical-reactivity. J Am Chem Soc 115:9148–9159
20. Program PETRA can be tested on the website http://www2.chemie.uni-erlangen.de/software/petra and is developed by Molecular Networks GmbH,http:www.mol-net.de
21. Zhang Q, Aires-de-Sousa J (2005) Structure-based classification of chemical reactions without assignment of reaction centers. J Chem Inf Model 45:1775–1783
22. Sabet R, Fassihi A (2008) QSAR study of antimicrobial 3-hydroxypyridine-4-one and 3-hydroxypyran-4-one derivatives using different chemometric tools. Int J Mol Sci 9:2407–2423
23. Loncle C, Brunel J, Vidal N, Dherbomez M, Letourneux Y (2004) Synthesis and antifungal activity of cholesterol-hydrazone derivatives. Eur J Med Chem 39:1067–1071
24. Melnyk P, Leroux V, Sergheraert C, Grellier P (2006) Design, synthesis and in vitro antimalarial activity of an acylhydrazone library. Bioorg Med Chem Lett 16:31–35
25. Kuecuekguezel S, Rollas S, Kuecuekguezel I, Kiraz M (1999) Synthesis and antimycobacterial activity of some coupling products from 4-aminobenzoic acid hydrazones. Eur J Med Chem 34:1093–1100
26. Dhar D, Taploo C (1982) Schiff bases and their applications. J Sci Ind Res 41:501–504
27. Przybylski P, Huczynski A, Pyta K, Brzezinski B, Bartl F (2009) Biological properties of schiff bases and azo derivatives of phenols. Curr Org Chem 13:124–148
28. Todeschini R (2010) Milano Chemometrics and QSPR Group. http://michem.disat.unimib.it/. Accessed 14 March 2010
29. Haaland D, Thomas E (1988) Partial least-squares methods for spectral analyses. 1. Relation to other quantitative calibration

methods and the extraction of qualitative information. Anal Chem 60:1193–1204
30. Kuzmanovski I, Novic M (2008) Counter-propagation neural network in Matlab. Chem Intell Lab Sys 90:84–91
31. Harris RLN (1976) Potential wool growth inhibitors. Improved syntheses of mimosine and related 4(1*H*)-pyridones. Aust J Chem 29:1329–1334
32. Sabet R, Behjati M, Vahabpour R, Memarnejadian A, Rostami M, Fassihi A, Aghasadeghi MR, Saghaie L, Miri R (in press) Int J Cardiol. doi:10.1016/j.ijcard.2011.11.067
33. Kirilmis C, Ahmedzade M, Servi S, Koca M, Kizirgil A, Kazaz C (2008) Synthesis and antimicrobial activity of some novel derivatives of benzofuran: part 2. The synthesis and antimicrobial activity of some novel 1-(1-benzofuran-2-yl)-2-mesitylethanone derivatives. Eur J Med Chem 43:300–308
34. de Souza SM, Delle Monache F, Smania A Jr (2005) Antibacterial activity of coumarins. Z Naturforsch 60:693–700